AIAA 81-0627R

Evaluation of Bonding Parameters on Random Fatigue Life of Bonded Aluminum Joints

H.F. Wolfe* and C.L. Rupert†
Flight Dynamics Laboratory, AFWAL, WPAFB, Ohio
and
H.S. Schwartz‡
Materials Laboratory, AFWAL, WPAFB, Ohio

Eighteen adhesively bonded aluminum coupons were tested on a vibration shaker at room temperature to determine the effects of varying the adhesive type/thickness, primer, and adherend surface preparation on their random bending fatigue life. Most of the fatigue failures occurred within 10^6 to 10^7 cycles, all at 900 microstrain. While neither the primer thickness nor the surface treatment seemed to influence the overall results, the coupons with thicker adhesive had a noticeably shorter fatigue life. Fractographic analyses of the failed adhesive surfaces showed the locus of fracture for all coupons was predominantly within the adhesive. The nitrile phenolic adhesive demonstrated a better fatigue resistance than the nitrile epoxy.

Introduction

THE development of durable high strength adhesives led to increased interest in applying bonding technology to aircraft structures. The benefits of bonding structures include increased fatigue life, improved fail-safe capabilities, and lowered manufacturing costs. Cost studies determined that the high costs in airframe construction are due to the large number of holes and fasteners required and the time required to assemble the parts. Adhesive joining of components can save both weight and cost by reducing the number of parts required.

Background

Sonic fatigue failures in riveted structures resulted in unacceptable maintenance and inspection burdens associated with aircraft operations. In some cases, sonic fatigue failures resulted in a major redesign effort of the structural components. The phenomenon manifests itself as fatigue cracks in skin panels, ribs, spars, stringers, and longerons. These fatigue failures result from the vibratory response of the structure to high intensity noise. Noise sources include jet propulsion noise, turbulent boundary-layer noise, separated flow noise, flow impingement, and scrubbing flow effects. These noise sources produce a fluctuating pressure field which excites various structural modes. The resonant response of these structures to fluctuating pressure fields produces a very rapid stress reversal which will result in fatigue failure if the stress reversals are of sufficient magnitude.

Fatigue data are needed for adhesively bonded structural designs to determine the life of the joint as a function of the magnitude of the stress levels. These data form the basis for the design criteria needed to determine the sonic fatigue life of adhesively bonded structures and to prevent premature structural failure from acoustic excitation.

The Materials Laboratory (ML) and the Flight Dynamics Laboratory (FDL) of the Air Force Wright Aeronautical Laboratories (AFWAL) conducted several research and development programs investigating adhesives, including their manufacturing processes, structural properties, and application to adhesively bonded aluminum structures. This paper describes a test and evaluation program to determine the effects of adhesive thickness, primer thickness, and the type of oxide layer on the random bending fatigue life sensitivity of an adhesively bonded metallic joint.

Testing Approach

Since many of the factors that affect sonic fatigue life of a structure are not analytically predictable, design criteria are developed using an empirical approach. A broad base of general design information in the form of nomographs, using both analytical and empirical approaches, was developed and summarized in "Sonic Fatigue Design Guide for Military Aircraft."[1] The procedures for predicting the sonic fatigue life of a structure is to determine the acoustic loads, the fundamental mode frequency, the maximum root mean square (rms) stress at a reference position, and the number of cycles (N) to failure from an appropriate S-N curve.

S-N curves were developed for various riveted configurations by using simple panels in an acoustic test facility. The panel construction was identical to the aircraft structural component of interest and subjected to an acoustic load under laboratory conditions which very closely simulate the acoustic field produced in service by the aircraft. A simple and less costly approach is to test a cantilever beam coupon section of the panel, including the joint on a vibration shaker. The panel and coupon data are then correlated to determine their relationship.

The narrow-band random amplitude vibration testing of simple structural joint samples for the purpose of generating fatigue design data for aircraft structures is an accepted practice. These data are considered as supplemental data to acoustic fatigue tests, as they are used to define a fatigue curve for a particular joint.

Previous Investigations

Previous investigations of weldbonded aluminum structures and various adhesively bonded aluminum structures are summarized in Ref. 2. The structures tested consisted of both panels and cantilever beam coupons. Several types of fatigue failures were obtained from these tests; however, one consistent predictable failure mode must be produced in order to develop an S-N curve from which the fatigue life can be

Presented as Paper 81-0627 at the AIAA Dynamics Specialists Conference, Atlanta, Ga., April 9-10, 1981; submitted April 24, 1981; revision received June 22, 1981. This paper is declared a work of the U.S. Government and therefore is in the public domain.

*Technical Manager, Acoustics and Sonic Fatigue Group.
†Aerospace Engineer, Acoustics and Sonic Fatigue Group.
‡Materials Research Engineer, Composites, Adhesives and Fibrous Materials Branch.

predicted. The failures in the adhesive bond system were classified as either cohesive or adhesive failures by visual inspection without magnification. A cohesive bond failure is defined as one in which part of the adhesive remains on both adherends after failure. An adhesive bond failure is defined as a complete separation of the adhesive from one adherend while remaining on the other adherend. Generally, adhesive failures are considered undesirable. A much lower fatigue strength resulted from adhesive failure mode than the cohesive failure mode. Also, the life of the adhesive failure mode is generally more unpredictable. Many of the failures could not be clearly identified as either "cohesive" or "adhesive" failures. Portions of the bond areas in some of the test structures exhibited both.

Most of the cantilever beam coupons were tested only until the fatigue crack propagated part way through the bond area. The bond area was examined after static loading the adhesive joint until it completely separated. It could be seen that initial cracking in the adhesive under dynamic loading was different from that produced by the static pull. The static pull generally was characterized by a separation midway through the thickness of the adhesive film; whereas, under dynamic load, the adhesive separated closer to the surface of the adherend.

Another area of concern was quality control, since different results often were obtained when the test structures were fabricated by different manufacturers using the same standards. Therefore an investigation was conducted of the adhesive/primer systems used in the Primary Adhesively Bonded Structural Technology (PABST) program sponsored by the Flight Dynamics Laboratory. These included adhesive/primer systems with phosphoric acid anodized aluminum adherends: FM73/BR127, M1133/BR127, AF55/XA3950, and EA9628/EA9202.

The FM73/BR127 with the surface preparation according to Boeing specification BAC5555 was then selected for more detailed investigation. Consequently, a follow-on program was conducted to evaluate 18 cantilever beam coupons and ten acoustic panels using this bond system. The fractured adhesive surfaces were evaluated using a scanning electron microscope (SEM) which indicated that the coupon failures were cohesive and essentially in the primer near the adhesive/primer interface. An evaluation of a panel fabricated at the same time indicated that the failure was cohesive within the primer on the skin close to the upper surface of the phosphoric acid anodize layer. In both cases, behavior of the primer became the principal concern.

The fatigue lives of the beam coupons were not noticeably different from those of the previous tests where detailed inspections of the fracture surfaces were not performed. The questions remaining unanswered from the previous investigations are how the adhesive thickness, primer thickness, and the type of oxide layer affect the fatigue life of the joint.

Shaker Test Specimen Description

The baseline materials and processes used in this investigation represent those used in the Air Force PABST program with Douglas Aircraft Company. In the PABST program, a section of a fuselage structure of a transport aircraft was designed, fabricated, and tested. The generic design of the PABST structure consisted of tees and longerons adhesively bonded to the skin with frames mechanically fastened to the tees. The skin was 2024 T-3 (bare), the tees 7075 T-6 (bare), the surface treatment phosphoric acid anodize, and the adhesive/primer system FM73/BR127. The FM73 adhesive is a nitrile rubber modified epoxy film and the primer consists of an epoxy phenolic resin in organic solvent with particulate inorganic chromate as the corrosion inhibitor. The baseline skin/tee specimens used in this investigation (group A) used these same materials and processes. Also, the same specific values for important material and process parameters, such as primer thickness, adhesive layer thickness, and surface preparation, were used. The test specimens were fabricated in the AFWAL Materials Laboratory. Dimensions of the test specimens are shown in Fig. 1.

In addition, three groups of specimens (groups B, C, and D) were fabricated, using the PABST material and process technology, but with the primer thickness and adhesive layer thickness different from those used in the PABST program. A fifth group of specimens (group E) was fabricated using the FM73/BR127 adhesive/primer system, but with the Forest Product Laboratories' (FPL) etch surface treatment instead of phosphoric acid anodize. A sixth group of specimens (group F) was fabricated using the AF30/EC1660 adhesive/primer system, which is a nitrile rubber phenolic type. A listing of the six sets of specimens, showing the adhesive/primer type, adhesive thickness, primer thickness, and surface treatment used, is shown in Table 1. Three specimens per group were prepared and tested, making a total of eighteen specimens.

The reason for investigating variations in the FM73/BR127 systems was to determine to what extent they influenced the initiation and propagation of interfacial and cohesive fracture. The AF30 adhesive was selected in this program as an adhesive having a lower modulus of elasticity and higher strain-to-fracture than FM73 adhesive. It was anticipated that these characteristics might make it more suitable to withstand the oscillating peel stresses caused by acoustic loads.

The first step of processing and fabrication was to surface treat the adherends using specification BAC5555 for the

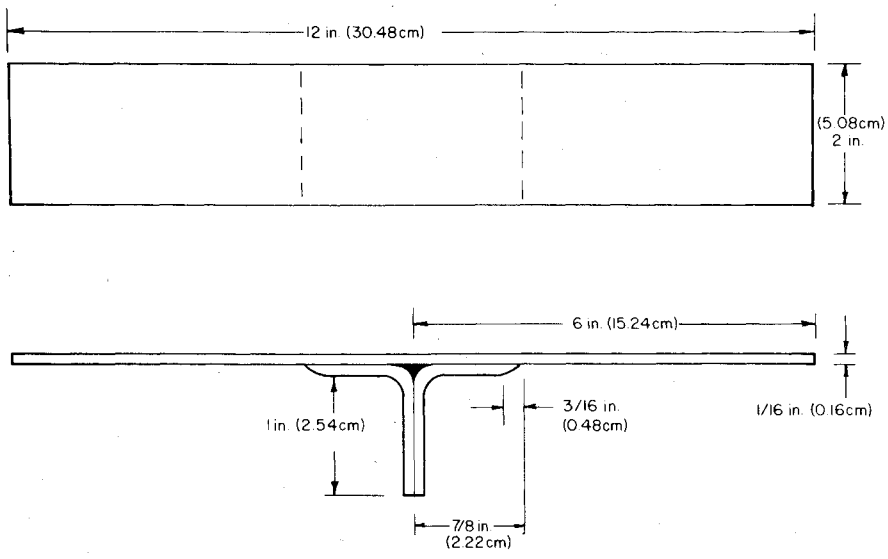

Fig. 1 Dimensions of beam coupons.

Table 1 Bonded aluminum coupon numbers

Group no.	Designation of adhesive/primer	Cured adhesive layer thickness, in. (cm)	Primer thickness, in. (cm)	Surface preparation Phosphoric acid anodize	Surface preparation FPL etch
A	FM73/BR127[a]	0.007 (0.018)	0.0003 (0.00076)	X	
B	FM73/BR127[a]	0.007 (0.018)	0.0001 (0.00025)	X	
C	FM73/BR127[a]	0.026 (0.066)	0.0001 (0.00025)	X	
D	FM73/NONE[a]	0.008 (0.020)	None	X	
E	FM73/BR127[a]	0.007 (0.018)	0.0001 (0.00025)		X
F	AF30/EC1660[b]	0.010 (0.025)	0.0003 (0.00076)		X

[a] Product of American Cyanamid Company. [b] Product of 3M Company.

phosphoric acid anodize and BAC5514 for the FPL etch. Then, primer was applied from a nitrogen pressurized spray gun, air dried and heat cured. After film adhesive was laid between the tee flange and the skin, the assembly was enclosed in a vacuum bag and cured in an autoclave according to the adhesive manufacturer's recommended cure cycle.

Two measures were taken in order to assure the quality of the fabricated specimens. One was to fabricate companion lap shear and wedge test panels, along with the skin/tee panels, for subsequent tests. The other was to perform nondestructive inspection of the bond line of the skin/tee specimens using ultrasonic attenuation and x-ray.

The lap shear specimens, tested at room temperature, met the strength requirements. The wedge specimens, exposed to 140° F (60°C) at 100% relative humidity, met the crack extension requirements, except for groups B and C. These specimens had a lower primer thickness than normal. This behavior was anticipated, since the primer thickness was about half that considered acceptable from a durability standpoint. However, as this program was to investigate the primer thickness for its effect on structural behavior rather than durability, the poor wedge test results were not considered a basis for rejecting the skin/tee specimens for fatigue testing. The ultrasonic and x-ray inspections of the bond lines did not reveal any significant flaws or anomalies in any of the skin/tee specimens.

Fatigue Tests

The double cantilever beam coupons were clamped at the midspan stiffener to a vibration shaker, shown in Fig. 2. These tests were conducted in the AFWAL Flight Dynamics Laboratory. A low level frequency sweep was made of each coupon to determine its resonant frequency. Damping measurements were accomplished using the log decrement method. This technique depends upon measuring the amplitude rate-of-decay of the coupon vibrating at its fundamental resonant frequency after abruptly cutting off the exciting force. The damping ratios (C/C_c) for each of the six coupon groups are summarized in Table 2. The five groups (A, B, C, D, E) using FM73 adhesive all have damping ratios that are comparable, ranging from 0.00086 to 0.00121. The exception is group F, using the more pliable AF30 adhesive, which makes a noticeably "softer" bonded joint, with a corresponding increase in damping ability. This is reflected in the higher damping ratios for the AF30 adhesive which averaged 0.0165. It should be noted that the damping ratios for riveted structure usually fall within the range found with the FM73 adhesive.

The coupons were vibrated at resonance to generate alternating bending stresses in the beam until failure was observed. A failure was defined either as a separation in the bonded joint or as a skin crack that was visually detectable without magnification. The control strain gage was located along the bond line at the outboard edge of the stiffener, where the maximum cantilever bending stress was expected. To confirm this, the axial stress distribution across the bond line of one coupon was measured using four strain gages. The gage locations and the resulting strain distribution are presented in Fig. 3. It was shown that the maximum strain was measured at the edge of the stiffener which verified the positioning of the control gage.

A baseline strain level of 900 microstrain was selected for all coupons to provide a comparison with data from previous programs where tests were conducted at the same level. Whenever feasible, each specimen was fatigue tested in second-mode bending to enable the accumulation of stress cycles at a much higher rate than possible in the first mode. There were two exceptions to this during the testing. In one

Table 2 Bonded coupon damping factors

Coupon no.	C/C_c	Coupon no.	C/C_c
A-1	0.00087	D-2	0.00096
A-3	0.00086	D-3	0.00099
B-1	0.00121	E-1	0.00094
B-3	0.00092	E-2	0.00088
C-1	0.00106	E-3	0.0011
C-2	0.00098	F-1	0.0156
C-3	0.00097	F-2	0.0172
D-1	0.00097	F-3	0.0169

Table 3 Summary of bonded aluminum coupon fatigue test data

Coupon group no.	900 Microstrain Cycles-to-failure $\times 10^6$	Type of failure
A-1	4.68	Adhesive bond
A-2	2.68	Stiffener
A-3	4.93	Adhesive bond
B-1	4.57	Midspan skin
B-2	8.32	Midspan skin
B-3	4.64	Midspan skin
B-M-1	5.82	Skin
B-M-2	12.38	Adhesive bond
B-M-3	8.45	Skin
C-1	1.28	Adhesive bond
C-2	1.94	Adhesive bond
C-3	2.75	Adhesive bond
D-1	4.31	Skin
D-2	4.43	Skin
D-3	5.65	Skin and adhesive bond
E-1	6.13	Skin
E-2	5.72	Skin
E-3	11.34	Midspan skin/adhesive
F-1	2.94	Adhesive bond
F-2	4.64	Adhesive bond
F-3	2.74	Adhesive bond

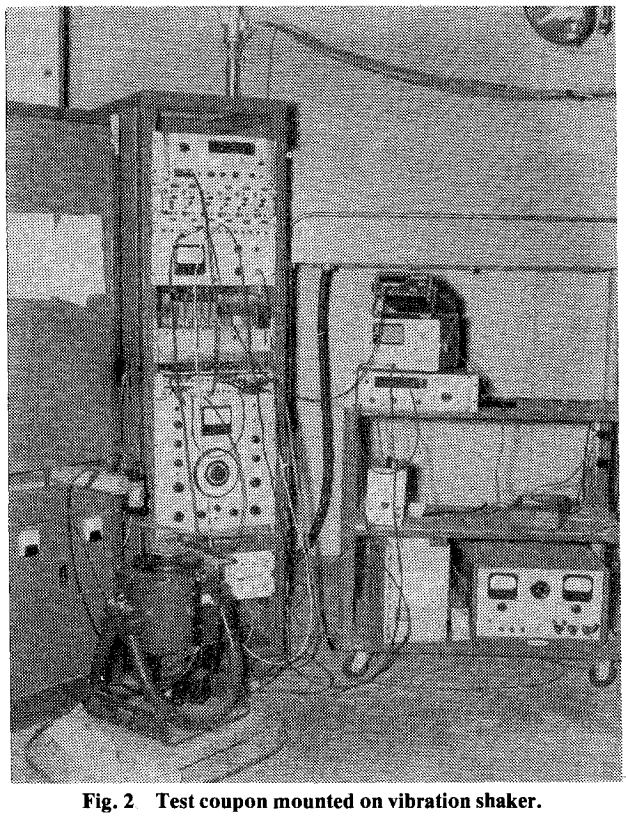

Fig. 2 Test coupon mounted on vibration shaker.

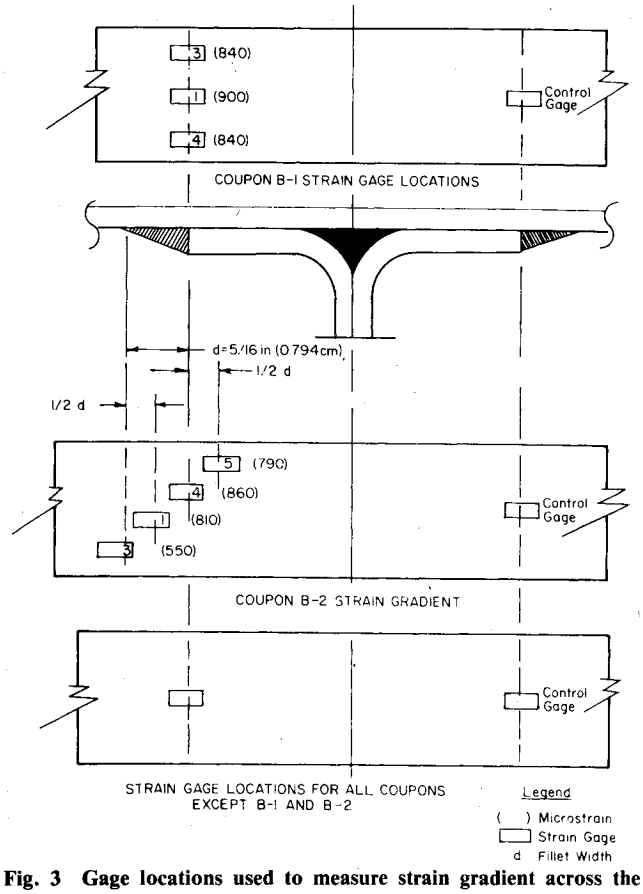

Fig. 3 Gage locations used to measure strain gradient across the bond line.

instance, the shaker acceleration capability was not sufficient to drive the group F nitrile phenolic coupons in the second mode at the required stress level of 900 microstrain. This was attributed to the "soft" skin-stiffener joint resulting from the AF30 adhesive, which is more pliable than the FM73. Consequently, the group F coupons were tested at their fundamental frequency, which required considerable less shaker head acceleration to attain 900 microstrain. The test results are summarized in Table 3. All three coupons that comprised group B experienced identical skin failures near midspan. Since no failures were evident in the adhesive, the test was continued by cutting off both ends of each group B coupon. The resulting beams, 3¾ in. long (9.525 cm) were tested in the first mode until failure was induced. These are identified as group B-M (modified).

Failure time was determined from visual inspection of each test coupon conducted at 2-3-h intervals, or whenever the coupon response frequency showed a noticeable decrease. When this point was reached, the test was terminated and the time-to-failure recorded. Figure 4 shows typical time histories of the frequency response. The exact time of crack initiation is not evident from these plots. The change in the slope of the frequency response vs time with the same bending load was not consistent. The beam coupons with the thicker adhesive failed much sooner. The resulting failure times are summarized in Table 3. The cycles-to-failure were obtained by multiplying the failure time by the modal frequency. Group B coupons failed at the midspan of the beam and were classified as skin failures. Further testing produced skin failures in two coupons and an adhesive failure in the third. A total of seven skin failures and 11 adhesive bond failures were obtained during this program. Most of the failures fell within 10^6 to 10^7 cycles. This scatter is normal for coupon testing at the same rms strain. The beam coupons with the thicker adhesive had somewhat shorter fatigue lives. Changes in the surface preparation and primer thickness did not produce a significant change in the fatigue life. Since conclusions drawn from a small number of fatigue failures can be misleading, these data were compared with the results from previous investigations and are identified herein as FDL/ML data. The skin failures compared very closely with the *S-N* curve developed in Ref. 2.

The time-to-failure of the adhesive in a bonded joint not only is a function of the strain in the surface of the coupon, but of the coupon thickness. Therefore, in previous investigations,[2] the strain data were converted to bending moment data to develop *M-N* (Bending Moment vs Cycles-to-Failure) curves which account for variations in beam thickness. Computing the bending moments from the strain permits the data to be presented on one curve for all thicknesses.

Figure 5 shows the 11 new adhesive fatigue failures (FDL/ML data) compared to previous data obtained from FM73 and AF55 adhesives. The dashed lines were constructed through the outlying points of the previous data and are parallel to the previously established *M-N* curve. Most of the new data fell within these outliers established from the previous data. A new *M-N* curve was then constructed from the FDL/ML data through the average value of the fatigue failures and parallel to the previous *M-N* curve. For a given bending moment, an increase in life by a factor of approximately 20 can be expected using the *M-N* curve developed with the FDL/ML fatigue failures.

Figure 6 shows the FDL/ML data and the *M-N* curve developed using the combined PABST, baseline bonded and weldbonded data.[2] The *M-N* curve for the FDL/ML data was constructed through the average value of the fatigue failures and parallel to the previous combined curve. For a given bending moment, it is shown that an increase in life by a factor of approximately 30 can be expected with the *M-N* curve developed with the FDL/ML fatigue failures.

The shaker beam tests determined the life of the bonded joint for each adhesive at a particular strain level on the surface of the beam. While the fatigue life for the more pliable AF30 coupon at 900 microstrain was comparable with FM73, a much higher excitation force was required to

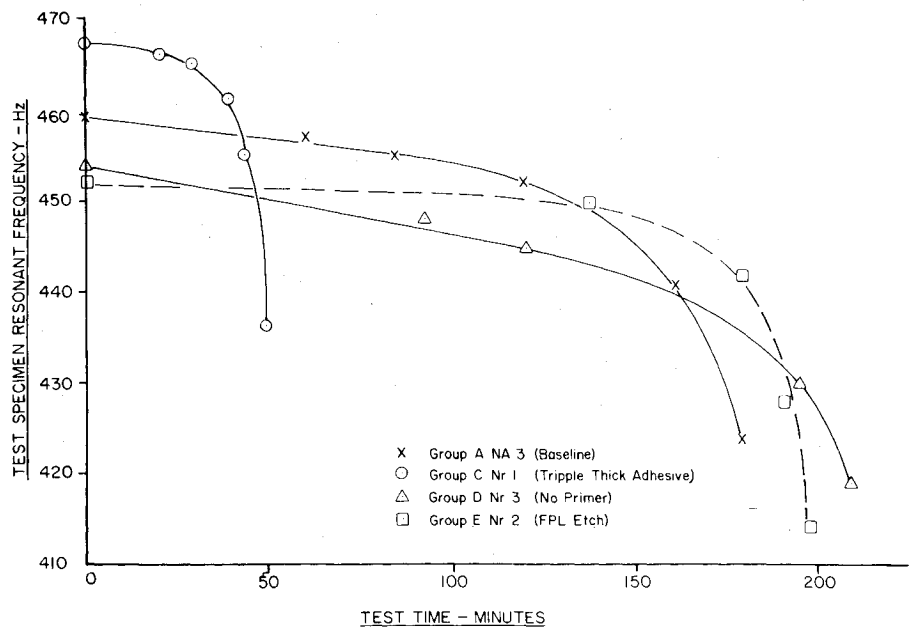

Fig. 4 Change in resonant frequency vs time.

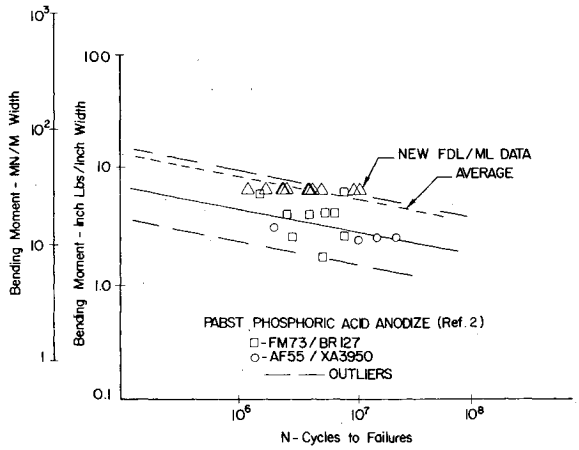

Fig. 5 Comparison of FDL/ML bond failures with PABST data.

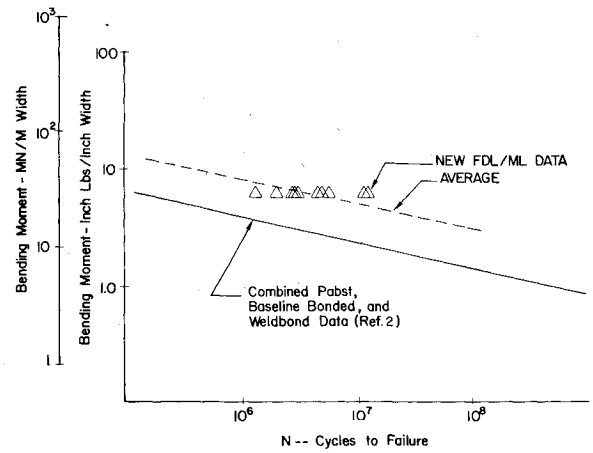

Fig. 6 Comparison of FDL/ML bond failures with combined PABST, baseline, and weldbond data.

produce the same strain in the AF30 coupon for the same excitation mode. Therefore, if an acoustic test was conducted with panels fabricated using these two adhesives at the same sound pressure level, it is expected that the skin stresses in the panel fabricated with the AF30 adhesive would be much lower. This decrease in the skin stresses would increase the sonic fatigue life of the structure. The damping data obtained from the AF30 coupons indicated a significantly higher damping ratio than those obtained from the FM73 adhesive. This also tends to increase the sonic fatigue life.

Fractographic Investigation of Skin/Tee Specimens after Failure

After each specimen had been fatigue tested, the propagation of the debond from the edge of the tee flange inward was typically about ⅜ in. deep. It was decided to perform fractographic investigations, using a scanning electron microscope (SEM) on the fracture surfaces which had debonded during testing.

To accomplish this, it first was necessary to separate the remaining bonded area of the specimen without changing the character of, or contaminating, the initial fracture surface. A file mark was made on the edge of the specimen where the fatigue fracture appeared to stop to clearly differentiate that part of the fracture surface created during fatigue testing from that part created by cleaving the remaining bonded portion. The specimen was then immersed in liquid nitrogen for several minutes and the remaining bond was pried apart. This was done by gripping the upstanding leg of the tee and the portion of the skin beyond the bonded area, to make sure the fracture surfaces were not touched. This procedure avoided excessive deformation of the adherends, since the adhesive became brittle enough to readily cleave. The mating fracture surface portions of the specimen from both skin and tee were cut off and prepared for SEM examination by vacuum coating with carbon. One representative specimen from each of the six groups was used in the fractographic investigations.

The objectives of the fractographic investigations were to determine the locus of fracture and the fracture mechanism. The preferred locus of fracture is cohesive (totally within the adhesive layer) because this type of fracture is predictable from measurable properties of the adhesive. In actual practice, fractures can also occur within the primer or the aluminum oxide layer, or at the adhesive/primer, primer/oxide, or oxide/aluminum interfaces.

The adhesives, primers, and oxide layers investigated in this program have distinct morphological features which are easily distinguishable in the scanning electron microscope. Therefore the determination of locus of fracture was a relatively straightforward matter. For example, the FM73

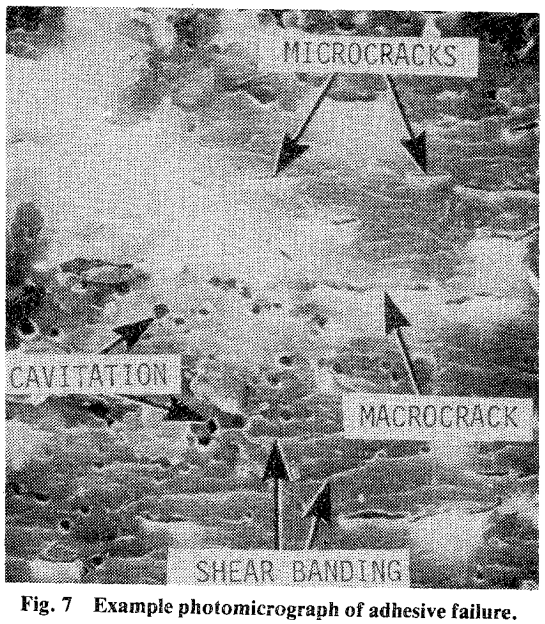

Fig. 7 Example photomicrograph of adhesive failure.

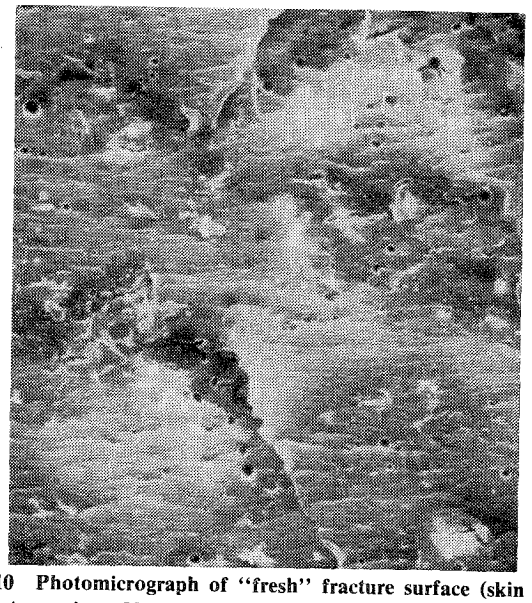

Fig. 10 Photomicrograph of "fresh" fracture surface (skin side), group A, specimen No. 1.

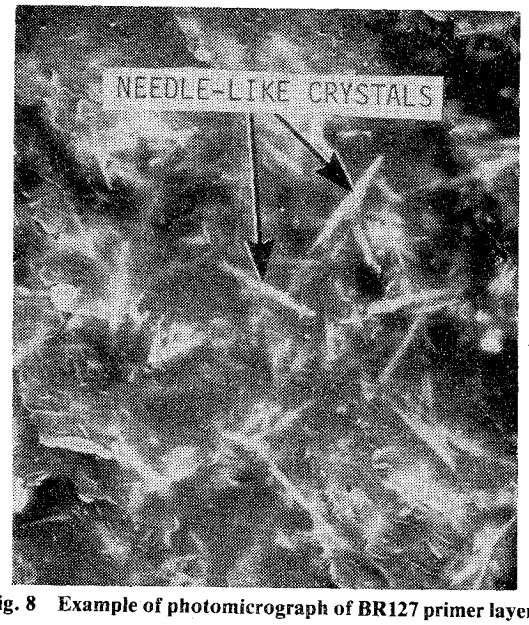

Fig. 8 Example of photomicrograph of BR127 primer layer.

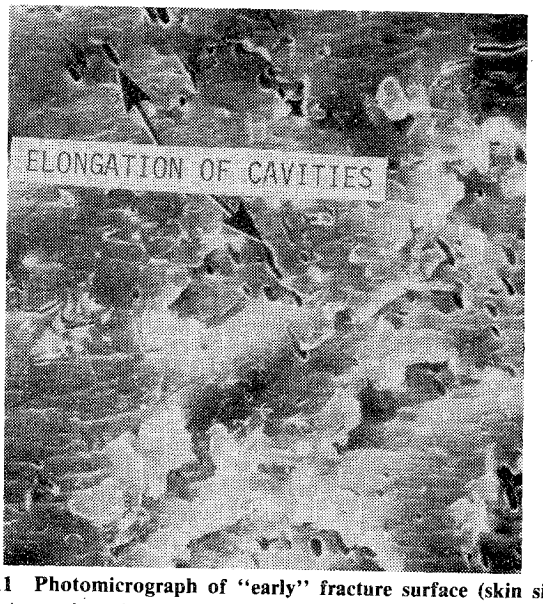

Fig. 11 Photomicrograph of "early" fracture surface (skin side), group A, specimen No. 1.

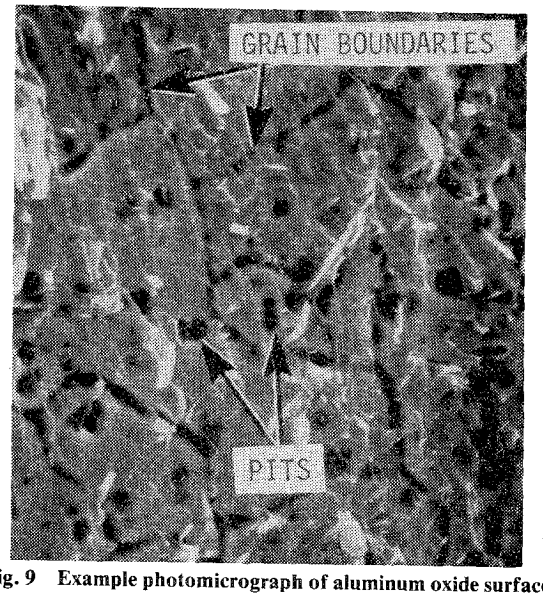

Fig. 9 Example photomicrograph of aluminum oxide surface.

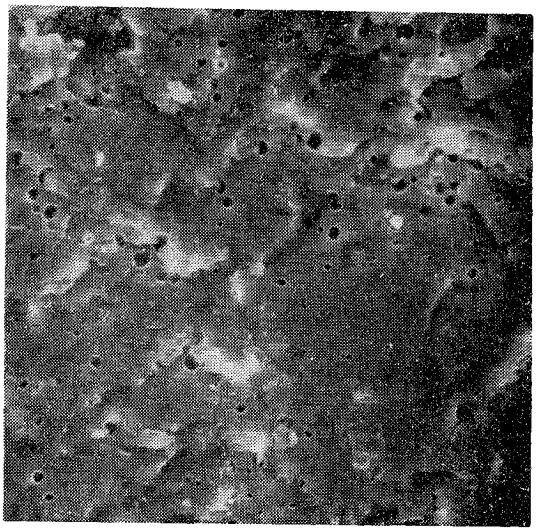

Fig. 12 Photomicrograph of fracture surface (tee side), group C, specimen No. 2.

adhesive is a two-phase material, consisting of elastomeric particles (precipitated during the curing reaction) in an epoxy continuum. Background information on the morphological and fracture characteristics of these types of two phase elastomer modified epoxies is given in Ref. 3, 4, and 5. Under combined shear and tensile loading such as the adhesive was subjected to in the fatigue tests, the adhesive fractures by cavitation around the elastomeric particles and by "shear banding," which has the appearance of thin layers, displaced stepwise from each other. Under repetitive loading or increasing magnitude of load, cracks form around these cavities, the cracks coalesce together forming macrocracks, and then gross fracture occurs. An example of such "cohesive" fracture is shown in Fig. 7.

The BR127 primer, used in conjunction with FM73 adhesive, contains a chromate corrosion inhibitor in the form of needlelike crystals. This gives the primer layer (and interfacial regions incorporating the primer) a distinctive, easily recognizable appearance, as shown in Fig. 8.

The aluminum oxide surface can be recognized by grain boundaries and pitting in the surface, as shown in Fig. 9. This particular photomicrograph of the fracture surface of a primed adhesive bonded specimen shows a very thin layer of primer polymer adhering to the oxide surface. (This photomicrograph is of a fracture surface of a different adhesive/primer system from that investigated in this program and is included only to illustrate this specific type of fracture.)

In addition to defining locus of fracture in the skin/tee specimens, the other objective of the fractographic investigations was to determine the "efficiency" of the fracture process. The term "efficiency" is used here to describe the degree to which the energy dissipation processes come into play during fracture. For example, combined cavitation, microcracking, and shear-banding mechanisms for FM73 represent a high efficiency fracture process.

In observing the fracture surfaces of the skin/tee specimens, the fractures were predominantly cohesive and the fracture processes were efficient in that they involved multiple mechanisms. In some cases locus of fracture was very close to the primer but, even in these cases, there was still a thin layer of adhesive adhering to the primer. The following discussion describes features of representative photomicrographs made of the fracture surfaces.

For the standard PABST material system (group A, specimen No. 1), fracture was typically cohesive but very close to the primer on the tee. This was indicated from a series of photomicrographs of fracture surfaces, several of which are shown for illustrative purposes. Figure 10 shows the fracture surface of the skin side, clearly revealing the classical cavitation and shear-banding typical of FM73 adhesive. There is little evidence of primer on the fracture surface except for small regions at the upper left and lower right. Figure 8 (previously referred to as illustrating a representative chromated primer surface) shows the mating fracture surface of the tee. The needlelike crystals of the chromate primer are very prominent. A thin layer of adhesive adhered to the primer, as clearly evidenced by the microcavitation in this layer. Therefore the net conclusion was that fracture occurred in the adhesive very close to the primer on the tee.

The fracture shown in Fig. 10 is immediately adjacent to a region which was intact (still bonded) when the fatigue test was terminated and, therefore represents a "freshly fractured" surface. The fracture surface in Fig. 11 is about ⅛ in. (0.318 cm) further outboard (away from the tee) from that shown in Fig. 10. Here, fracture occurred earlier since it was subjected to greater dimensional excursion. This caused elongation of the cavities and subsequent microcracks connecting the cavities.

For a specimen from group C (specimen No. 2, the PABST system, but with three layers of adhesive and a thinner than normal primer), the locus of fracture was predominantly

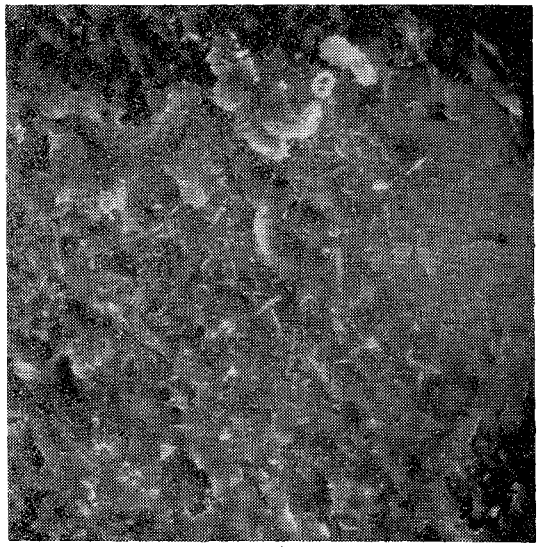

Fig. 13 Photomicrograph of fracture surface (skin side), group C, specimen No. 2.

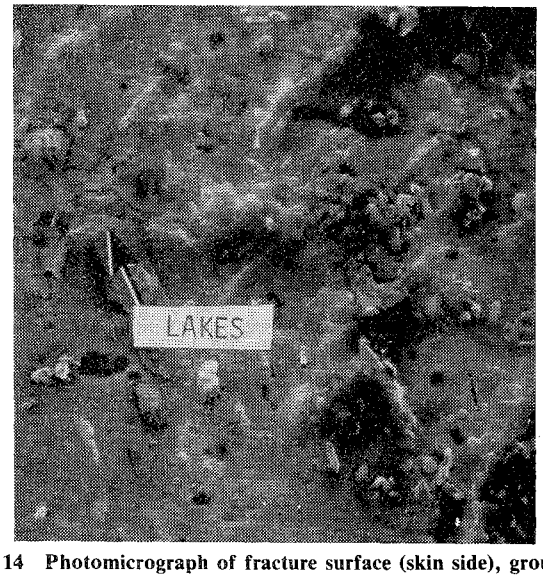

Fig. 14 Photomicrograph of fracture surface (skin side), group D, specimen No. 3, near initiation 500X.

cohesive within the adhesive, but there were also zones of interfacial failure, namely, adhesive-to-primer failure, and primer-to-oxide failure. The interfacial failures were on the skin side. This is illustrated by Fig. 12 for the tee and Fig. 13 for the skin, both showing fracture surfaces near the zone of fracture initiation. Figure 12 shows the classical cohesive failure for FM73, whereas Fig. 13 shows a combination of failure modes, both cohesive and interfacial.

For a representative specimen from group D (specimen No. 3, FM73 adhesive on phosphoric acid anodize without a primer), failure initiated cohesively but then propagated interfacially toward the skin. Figure 14 shows the fracture surface of the skin about ⅛ in. (0.318 cm) from the point of initiation. This photomicrograph at 500X, shows a thin layer of polymer adhering to the oxide. The pits in the adherend surface are evident, indicating that the fracture is very close to the oxide surface. One interesting feature in this photomicrograph is the presence of "lakes" of a dispersed phase in the polymer layer, rather than spherical particles. The reason for the lakes is not known. However, it is speculated that they may have resulted from the high surface energy of the aluminum oxide causing sufficient spreading of the adjacent polymer layer to transform the elastomeric

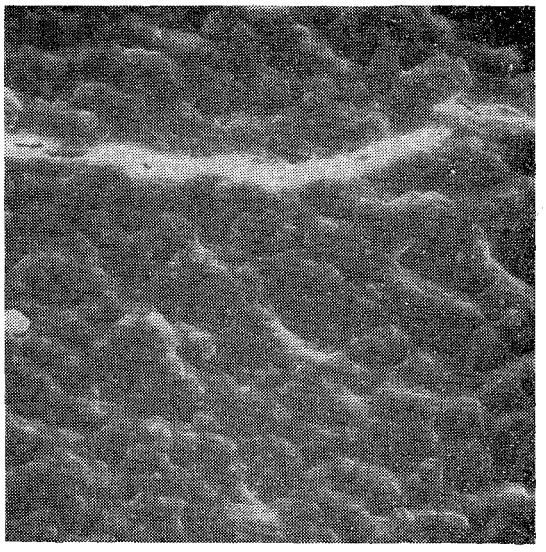

Fig. 15 Photomicrograph of fracture surface (skin side), group F, specimen No. 3.

Fig. 16 Photomicrograph of flash area.

second phase of the adhesive into a planar, rather than a spherical configuration.

Photomicrographs of the fracture surfaces of a specimen made with AF30 (group F, specimen No. 3), a nitrile rubber phenolic adhesive, indicated predominantly cohesive fracture, but with a morphology different from that of FM73 adhesive. Figure 15 of the fracture surface of the skin shows a continuous phase which appears to be elastomeric. The elastomeric nature is indicated by local regions of "necked-down" material and the undulating, highly deformed overlapping layers. Figure 16 is a photomicrograph of the flash area at the edge of the tee flange. The interesting features here are the fragmentation of the surface grains of the adherend and the separations at grain boundaries. This is presumed to have been caused by the very high energy input during the fatigue test.

The results of the fractographic investigations are summarized as follows:

1) Adhesion at interfaces (e.g., primer-to-adherend oxide and adhesive-to-primer) was generally maintained during the process of fracture propagation.

2) Fractures which visually appeared to be interfacial were usually near the primer-to-adhesive interface but, in most cases, had a thin layer of adhesive still bonded to the primer.

3) For both FM73 (nitrile rubber epoxy) and AF30 (nitrile rubber phenolic) adhesives, the morphology of cohesive fractures showed that the full spectrum of fracture processes, which these adhesives are capable of undergoing, were manifested.

Conclusions

The double cantilever beam coupon tests provided a means of generating consistent, reproducible sonic fatigue data for adhesively bonded aluminum structures of the sheet-stringer type. The fatigue data, using the FM73/BR127 adhesive/primer system, were essentially insensitive to variations in primer thickness and type of adherend surface treatment. The beam coupons with the thicker adhesive had somewhat shorter fatigue lives and showed evidence of a failure mode that accounted for it. A slightly longer random bending fatigue life was obtained with these beam coupons than with those previously tested. This was attributed to improved quality control used in the fabrication of these coupons.

The AF30 adhesive was selected in this program as having a lower modulus of elasticity and higher strain-to-fracture than FM73 adhesive. It was anticipated that, with these characteristics, it might better withstand the oscillation peel stresses due to acoustic loads. The damping data indicated that the AF30 adhesive has a significantly higher damping ratio than the FM73 adhesive. A much higher acceleration level was required to attain the desired strain level in the AF30 coupons than in the FM73 coupons. Since the AF30 coupons required more energy to reach a given strain level and have considerably higher damping properties at room temperature, it was concluded that a structure, using AF30 adhesive, would have a corresponding increase in sonic fatigue resistance at room temperature.

A failure analysis of the fractured surfaces was made using a scanning electron microscope (SEM). The failure analysis consisted of two types of observations, one being "locus-of-fracture" and the other being "fracture mechanisms." The locus-of-fracture observations determined whether fracture was within the adhesive, at the adhesive-to-primer interface, within the primer, at the primer-to-oxide interface, or within the oxide. The fractures observed, except for group C, which had interfacial failure, were essentially all within the adhesive; however, in some cases the failures were very close to the primer surface. Fractographic observations also determined the mechanisms of fracture initiation and propagation, and noted physical features that identified energy dissipation mechanisms during fracture.

References

[1] Rudder, F.F. Jr. and Plumbee, H.E. Jr., "Sonic Fatigue Design Guide for Military Aircraft," AF Flight Dynamics Laboratory, Wright-Patterson Air Force Base, Ohio, AFFDL-TR-74-112 (AD-B004-600L), May 1975.

[2] Wentz, K.R. and Wolfe, H.F., "Development of Random Fatigue Data for Adhesively Bonded and Weldbonded Structures Subjected to Dynamic Excitation," *ASME Journal of Engineering Material and Technology*, Vol. 100, Jan. 1978, pp. 70-76.

[3] Rowe, E.H., Seibert, A.R., and Drake, R.S., "Toughening Thermosets with Liquid Butadiene/Acrylonitrile Polymers," *Modern Plastics*, Aug. 1970.

[4] Rowe, E.H. and Riew, C.K., "What Failure Mechanisms Tell About Toughened Epoxy Resins," *Plastics Engineering*, March 1975.

[5] Drake, R. and Seibert, A., "Elastomer-Modified Epoxy Resins for Structural Applications," *SAMPE Quarterly*, Vol. 6, No. 4, July 1975.